UDK 66.096.4:629.3.018.4
Original scientific article/Izvirni znanstveni članek

ISSN 1580-2949
Mater. Tehnol.

# ANALYSIS OF DAMAGE IN LOW-VELOCITY IMPACT-TESTED GFRP-ALUMINUM HONEYCOMB SANDWICH PANELS USING MATLAB

# ANALIZA POŠKODB PO UDARCU Z MAJHNO HITROSTJO - PREIZKUS NA PANELIH S SENDVIČ STRUKTURO SATOVJA IZ GFRP-ALUMINIJ Z UPORABO PROGRAMSKEGA ORODJA MATLAB

**Prasanth Prabhakaran Vanaja[1,*], Jayaram Radhakrishnan Shanthi[2], Senthil Murugan Subramanian[3], Kanthavelkumaran Natesan[1]**

[1]Department of Mechanical Engineering, Ponjesly College of Engineering, Nagercoil, Tamil Nadu 629003, India
[2]Department of Mechanical Engineering, Amrita Vishwa Vidyapeetham, Nagercoil, Tamil Nadu 629901, India
[3]Department of Mechanical Engineering, Rajalakshmi Engineering College (Autonomous), Thandalam, Tamil Nadu 602105, India

*Prejem rokopisa – received: 2024-05-16; sprejem za objavo – accepted for publication: 2025-01-22*

doi:10.17222/mit.2024.1192

Honeycomb sandwich structures are widely utilized in civil infrastructure applications due to their exceptional mechanical properties. To assess their damage tolerance and strength, low-velocity impact (LVI) tests are commonly performed. This study investigates the damage tolerance of a polyester pin-incorporated foam-filled honeycomb sandwich panel (PFHS) through LVI experiments, comparing it to a conventional foam-filled honeycomb sandwich panel (FHS). The comparison focuses on damage assessment metrics such as damaged area and microscopic examination of the damaged surface. Due to indistinct colors and irregular shapes of damage of LVI-tested panels, visual inspection methods often struggle to accurately determine the damaged area. To address this limitation, this study introduces a cost-effective approach based on digital image analysis and MATLAB programming to precisely quantify the damaged area and assess damage severity without requiring advanced instrumentation. The proposed method proved to be efficient, with results closely matching those obtained through visual inspection. Furthermore, an addition of polyester pin reinforcement significantly enhanced the interlayer crack resistance of the foam-filled honeycomb sandwich panels, resulting in a notable reduction in the impact damaged area.

Keywords: debonding, low-velocity impact, sandwich, polyester pin, MATLAB, digital image analysis

Sendvič strukture v obliki satovja se veliko uporabljajo za aplikacije v civilni infrastrukturi zaradi odličnih mehanskih lastnosti. Pogosto se v praksi izvajajo na te vrste strukturah udarni testi z majhno hitrostjo (LVI; angl.: Low-Velocity Impact) zato, da bi se realno ocenilo njihovo mehansko trdnost in toleranco do poškodb. V tem članku avtorji opisujejo študijo s katero so ugotavljali toleranco do poškodb z LVI preizkusi poliesterskega trna združenega s sendvič panelnim satovjem napolnjenim s peno (PFHS angl.: Incorporated Foam-Filled Honeycomb Sandwich Panel). To panelno sendvič strukturo so avtorji primerjali s konvencionalnim sendvič satovjem (FHS; angl.: Foam-Filled Honeycomb Sandwich Panel). V primerjavi so se avtorji osredotočili na oceno poškodb po preseku in mikroskopske preiskave poškodb površine. Zaradi nejasnih barv in nepravilnih oblik poškodb na testiranih LVI panelih vizualni pregled pogosto ne daje prave slike o nastalih poškodbah po preseku in površini. Zato, da bi odpravili te pomanjkljivosti so avtorji v tej študiji uvedli cenovno učinkovit pristop s pomočjo digitalne analize slike in programiranja z orodjem MATLAB. S tem so bolj natančno ovrednotili poškodovan presek strukture in ocenili resnost nastalih poškodb, ne da bi za to potrebovali napredno inštrumentirano opremo. Avtorji v članku ugotavljajo, da je uporabljeni pristop učinkovit. Rezultati preiskave so blizu tistim, ki so bili dobljeni z vizualno preiskavo. Nadalje avtorji ugotavljajo, da se je trdnost poliesterskega trna z ojačitvijo močno izboljšala. Zaradi povečane odpornosti proti razpokam med posameznimi plastmi (angl.: interlayer crack resistance) s peno napolnjenega satovja sendvič panelov pa se je pomembno zmanjšalo tudi področje poškodovanega preseka.

Ključne besede: dekohezija, udarci z majhno hitrostjo, sendvič, poliester, trn, MATLAB, digitalna analiza slike

## 1 INTRODUCTION

Sandwich panels are widely used in a variety of engineering applications, including marine, wind energy, automation, and aircraft sectors, due to their high structural rigidity, high flexural strength, crashworthiness, and good thermal and acoustical properties. There is always a need for new, more effective materials. Consequently, research into honeycomb sandwich structures has grown substantially. Sandwich panels' primary benefits include their ability to increase stiffness without adding weight and their lower production costs.[1,2] A sandwich structure's top and bottom face sheets can withstand compression and tensile loads correspondingly, while the core material can withstand shear loads under bending loads. Contrarily, the primary weakness of this sandwich construction is that minor exterior impact "threats" from a tool drop or other foreign objects were determined to involve "low impact conditions" which can produce face sheet dent, leading to internal damage such as matrix cracking, fiber breaking, face/core debonding, and core crushing.[3] In this scenario, a visual examination may re-

*Corresponding author's e-mail:
findprasanth@gmail.com (Prasanth Prabhakaran Vanaja)

veal slight damage to the top facing, but severe damage may occur between the facings and the core. Additionally, low-velocity impact damage may result in a significant decrease in the sandwich structures' rigidity, and residual compressive strength leading to structural failure.[4] For a typical sandwich panel, the strength of the interfacial region is crucial to the overall performance of the sandwich construction because it combines heterogeneous materials, such as high-strength face sheets and low-density core material.[5]

Any fracture forming in the interfacial zone during in-service loading can cause the face sheets to separate from the core (debonding), greatly reducing the structure's load-bearing capacity and ultimately leading to catastrophic failure.[6] Many researchers have thoroughly studied the low-velocity impact response of sandwich panels made up of different facings and core materials. There have been numerous studies on the damage resistance and tolerance response of sandwich constructions exposed to low-velocity impact loads[7–9] and an enormous effort has been made to increase sandwich panels' impact resistance properties.[10–12] Among the constituents of sandwich panels such as facings and core, the material properties of the former are considered essential for increasing the impact resistance of sandwich panels.[13] Numerical studies on the failure processes (failure initiation and propagation) and the mechanism of sandwich panels under low-velocity impact have been done.[14] Through several experimental and computational studies, delamination and debonding were found to be the two of the most significant failures that can occur in sandwich panels.[15–17] The overall attributes of sandwich panels are reduced as a result of the interfacial debonding between the face and core, which causes local deformation through buckling. To improve the interfacial bonding between facings and core, various toughening techniques are used. Common toughening techniques include face-core Z-pinning, core alteration with perforations and grooves, stitching, tufting, and 3D weaving.[18–20]

Abdi et al.[21] studied the mechanical behaviour of a sandwich panel with a foam core and matrix pin reinforcement. They claimed that adding matrix pins to the foam to reinforce it significantly improves the out-of-plane compression, flexural and indentation properties. Additionally, the sandwich panels' structural and interface strength is improved by using matrix pinning to support or replace the existing core. Several studies have been carried out experimentally and numerically on the LVI response of matrix-pinned sandwich structures and reported that pinning prevents the progression of delamination, reducing damaged area and thereby increasing the load-carrying capability.[22,23] General matrix pinning-based interfacial toughening procedures are not viable since the core of honeycomb sandwich panels is a hollow metal. However, when the honeycomb core is stuffed with foam, it is doable. Also, a foam-filled core contains a larger area of contact with the facings than the unfilled core, which leads to improved resistance to the interface debonding and delamination.[24] In addition, the foam filling of the honeycomb core improves the interlaminar strength and damage tolerance of sandwich panels under LVI.[25]

Moreover, with the expansion of composite sandwich panel applications, locating and evaluating the damaged area is becoming an important and challenging issue. There are numerous ways to find and quantify the damaged area in composite sandwich panels. To determine the size, geometry, and location of the delamination area in a sandwich panel, non-destructive testing (NDT) using ultrasonic C-scan is frequently employed. The heterogeneous properties of sandwich panels result in the absorption and dispersion of sound waves, making data interpretation challenging. It takes expert knowledge and experience with composite sandwich panels to assess delamination.[26] C-scan overestimates the damage and only considers the region of overlapping delaminations immediately below the impact position, while visual assessment considers the size of the greatest single delamination. Infrared thermography, shearography, X-ray tomography, and other NDT techniques are among the others used to find damage in composite panels. These approaches are constrained for several reasons, including their high cost and poor detection efficiency.[27]

Many researchers calculated the damaged area value (maximum) by focusing just on the maximum length of the damaged area because the LVI test damages have random shapes. Although the undamaged area is also taken into account in research, the damaged area is determined using the greatest length of the damage zone as the diameter, from which the damaged area is then calculated. The exact damaged area is found using the suggested digital image analysis approach. This paper's innovation is the use of cutting-edge methods (image analysis), which allow for the calculation of the damaged area of an uneven shape. The suggested approach pinpoints the precise damaged region without taking the undamaged area into account. The objectives of this research are to perform an LVI test on a prepared AA3003 honeycomb sandwich panel with and without pin reinforcement with varying energy levels ranging from 10 J to 50 J, and to investigate damage assessments such as identification of a damaged area using MATLAB image processing and microscopic images of the damaged surface.

## 2 MATERIALS AND METHODS

An aluminium honeycomb with cells measuring 6.3 mm in diameter, 0.068 mm in wall thickness, and 10 mm in height was used as the core. Glass fiber with a plain weave and a surface density of 600 g/m$^2$ was used to create the face sheet, along with the polyester resin. The resin could be hardened and accelerated at room temperature in the presence of methyl ethyl ketone per-

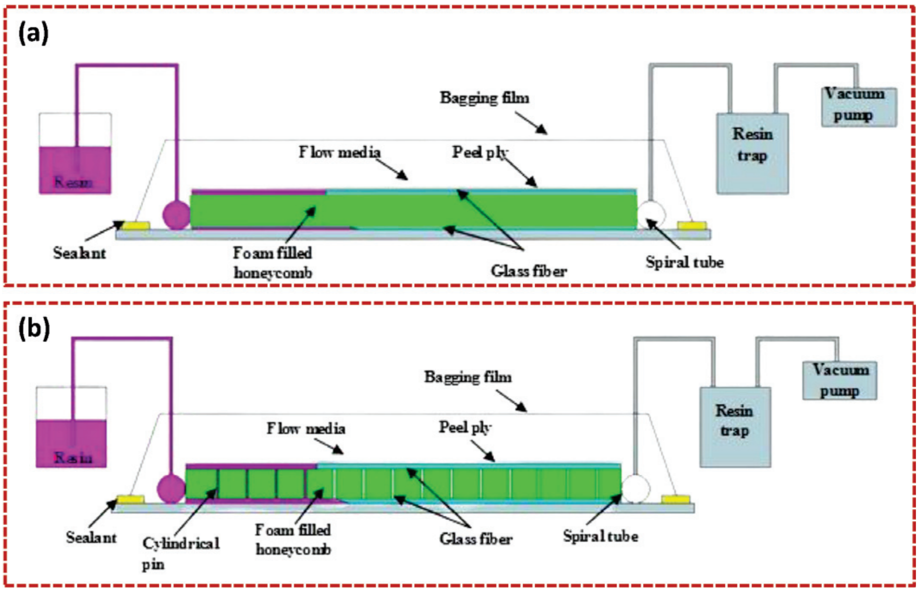


**Figure 1:** Diagrams illustrating the differences between the manufacture of (a) FHS panels and (b) PFHS panels, using the vacuum infusion method

oxide (MEKP) and cobalt naphthenate, respectively. A die with the required size was built to fill the honeycomb core with polyurethane foam. The honeycomb core was placed on top of the foam while in the solution state, with a tiny gap at the die's bottom. The honeycomb core was filled with foam after it had solidified, and the extra foam on top of the core was removed. The vacuum infusion approach was used to create FHS and PFHS panels. The schematics in Figures 1a and 1b illustrate how the vacuum infusion process differs in the manufacture of FHS and PFHS panels. The manufacturing was carried out using a method similar to the one described above.[28]

**Figure 2a** depicts the PFHS panel's schematic representation. The pins were produced using the polyester matrix utilized in the face sheets. Two types of PFHS panels were manufactured with two distinct pin diameters of 2 mm (PFHS2) and 3 mm (PFHS3) to assess their damage under LVI from 10 J to 50 J. The sandwich panel's core was strengthened, and the interface strength between the face and core was improved, using polyester pins. The face sheets, foam-filled honeycomb core, and polyester pins were all created as one, complete solid structure during a single manufacturing phase, which significantly shortened the manufacturing process. According to ASTM D5628-10 standard, low-velocity impact testing was performed on the prepared specimens (100 × 100 × 13) mm in the energy range of 10.0–50.0 J by adjusting the impactor's velocity.

The impactor used had a 12.7 mm diameter and weighed 2.926 kg. A sample was put in the testing machine fixture using a pneumatic actuation mechanism.

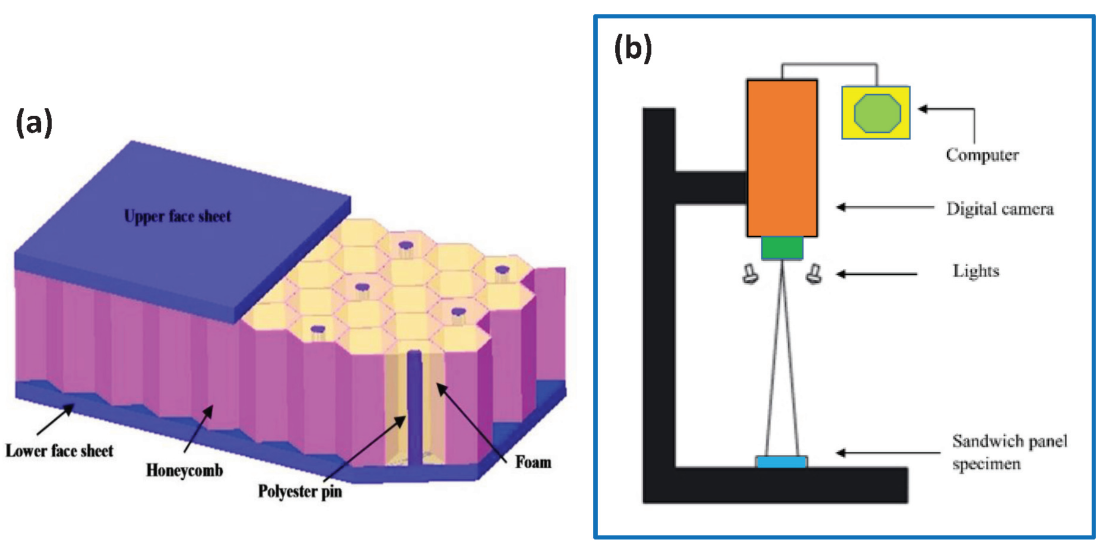


**Figure 2:** a) Schematic representation of the PFHS panel (face sheet partially removed to show the arrangement of pins), b) illustration of photographing a damaged specimen

The average of three tests was used. Using a Canon EOS 700D (Canon India Private Limited India) digital camera, the damage on a specimen was qualitatively determined following the low-velocity impact experiment. For evaluating an impact damaged area, an image processing technique based on MATLAB software (R2022b) was employed. The conceptual illustration for photographing a damaged specimen is shown in **Figure 2b**. The microscope was commonly used for inspecting component surfaces. Following the LVI test, microscopic images of the specimens were captured using a COSLAB (model: ZSM116) compound light microscope with image-capturing software.

## 3 RESULTS AND DISCUSSION

The results and discussions of the load and energy versus time curves, and the load versus deflection curve for sandwich panels subjected to impact energies of 10–50 J, are provided in the references.[29,30] The damaged area of each panel was determined using MATLAB image processing methods and, for comparison, the damaged area was also calculated using the visual inspection method. Due to the reflected light from the specimens' damaged area, which is used to determine the damaged area, the pixel value in the photograph is varied. The maximum damaged area is the maximum length of the damage taken into consideration as the diameter, as shown in **Figure 3a**. The exact damaged area is the irregular damaged area. As can be seen, both the damaged and undamaged portions are included in the damaged area, which is determined by the damage's maximum length expressed as the diameter. This restriction can be bypassed with the aid of image processing. **Figures 3b–3e** show various phases of the image processing method used to determine the damaged area from the impact damage image. In this instance, the depth of damage, also referred to as the damage severity, is given weight in addition to the damaged area. The processed image of the low-velocity impact-damaged specimen is divided into three groups based on the intensity of the pixels: severely damaged areas (red), moderately damaged areas (rose), and lightly damaged areas (green).

### *3.1 Comparison of damaged areas detected by IP and VI methods*

To compare the damaged areas estimated by image processing and visual inspection methods, the low-velocity impact-tested FHS sample was used. The damaged areas identified with image processing and visual assessment are shown in **Tables 1** and **2**. The damaged area discovered through visual assessment is higher than that determined using image processing. The visual evaluation method overestimates the value due to human error. The image processing approach compared the exact damaged area to the maximum damaged area. The žexact damaged area' refers to the precise impact-damaged region determined by MATLAB image processing. Unlike the maximum damaged area, which assumes a circular shape based on the longest diameter, the exact damaged area excludes undamaged portions within the boundary, providing a more accurate representation of the irregularly shaped damage. According to **Figure 4a**, the exact damaged area for the damaged specimen studied at different impact energies of 10–50 J is (40, 34.7, 32.2,

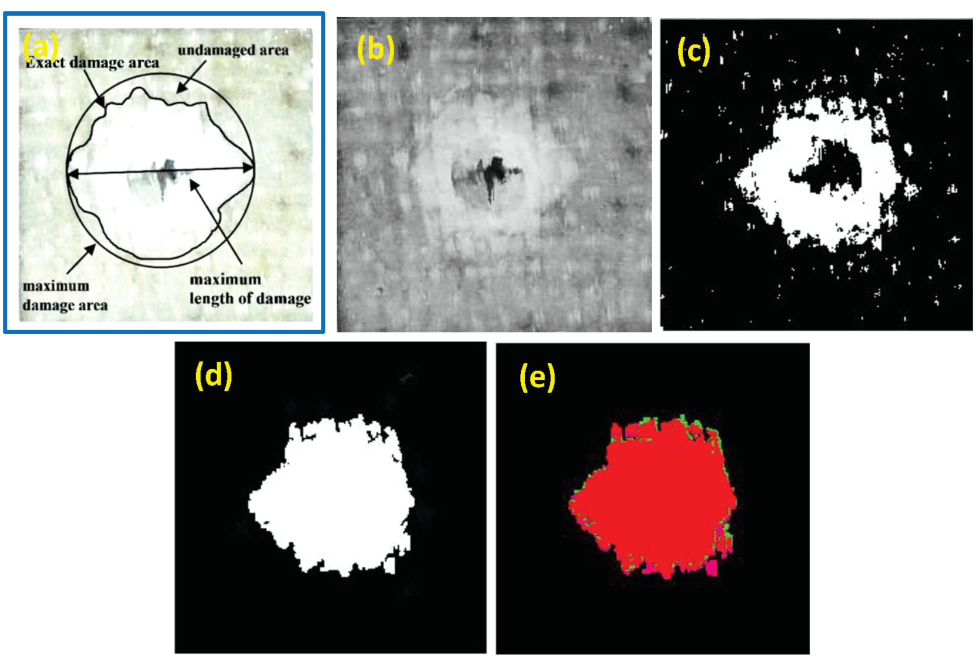


**Figure 3:** Impact damage images: a) difference between the maximum and exact damaged area, b) captured image, c–d) processing of the image, e) final image

**Table 1:** Comparison of damaged areas on the low-velocity impact-tested FHS specimen calculated using visual inspection and image processing

| Impact energy (J) | Visual inspection (VI) method | | Image processing (IP) method | |
|---|---|---|---|---|
| | Max. length of the damage, $D_v$ (mm) | Max. damaged area, $A_v$ (mm$^2$) | Max. length of the damage, $D_I$ (mm) | Max. damaged area, $A_I$ (mm$^2$) |
| 10 | 27.33 | 586.92 | 25.06 | 493.26 |
| 20 | 28.57 | 642.34 | 27.02 | 573.51 |
| 30 | 30.97 | 753.48 | 28.72 | 648.13 |
| 40 | 32.38 | 823.74 | 29.63 | 689.7 |
| 50 | 33.62 | 887.85 | 31.21 | 765.32 |

**Table 2:** Damaged areas on the low-velocity impact-tested FHS specimen calculated with the IP method

| Impact energy (J) | Exact damaged area, $A_E$ (mm$^2$) | Severely damaged area, $A_S$ (mm$^2$) | Medium damaged area, $A_M$ (mm$^2$) | Lightly damaged area, $A_L$ (mm$^2$) |
|---|---|---|---|---|
| 10 | 403.54 | 378.73 | 18.24 | 6.57 |
| 20 | 481.88 | 454.23 | 17.87 | 9.78 |
| 30 | 518.17 | 495.7 | 15.41 | 7.06 |
| 40 | 552.18 | 521.07 | 18.09 | 13.02 |
| 50 | 626.32 | 594.17 | 21.02 | 11.13 |

28.21 and 31.7) % lower than the maximum damaged area. The maximum length of damage represents the diameter, from which the maximum damaged area is determined, and within which the undamaged areas are also considered. The damaged area is mostly irregular in shape since it is not perfectly circular. The impact energy's effect on the impact-damaged areas of the FHS and PFHS panels is depicted in **Figure 4b**. The values of the damaged area based on the reflected light intensity are shown in **Tables 1** and **2**. Additionally, these values are displayed in **Figures 5a–5d** for FHS and PFHS panels as a function of impact energy. In addition to comparing specimens based on the damaged area, the severity of damage was taken into account. It is clear that when energy increases, the region that is severely, moderately, or

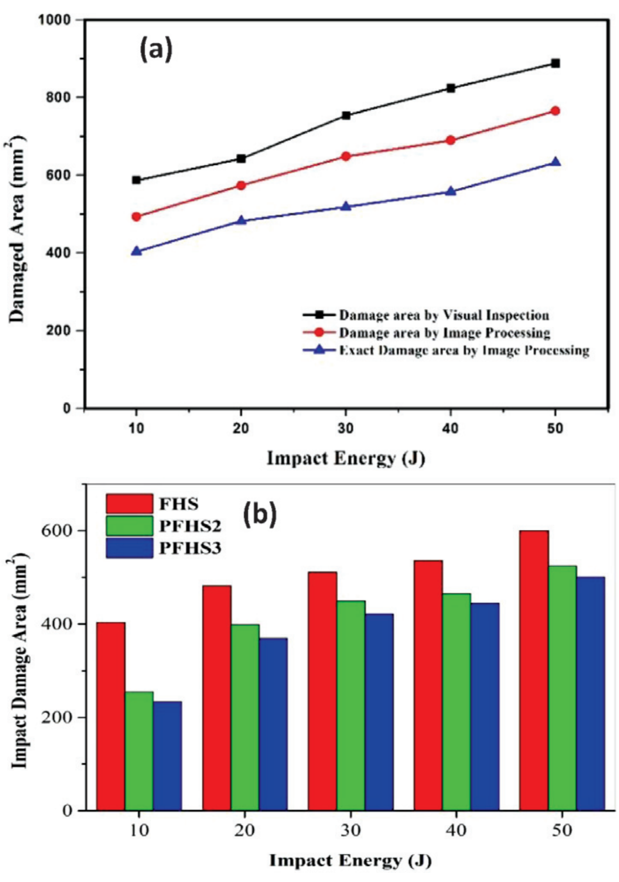


**Figure 4:** a) Damaged area measured with visual inspection and image processing (FHS), b) impact energy's effects on the damaged area of sandwich panels

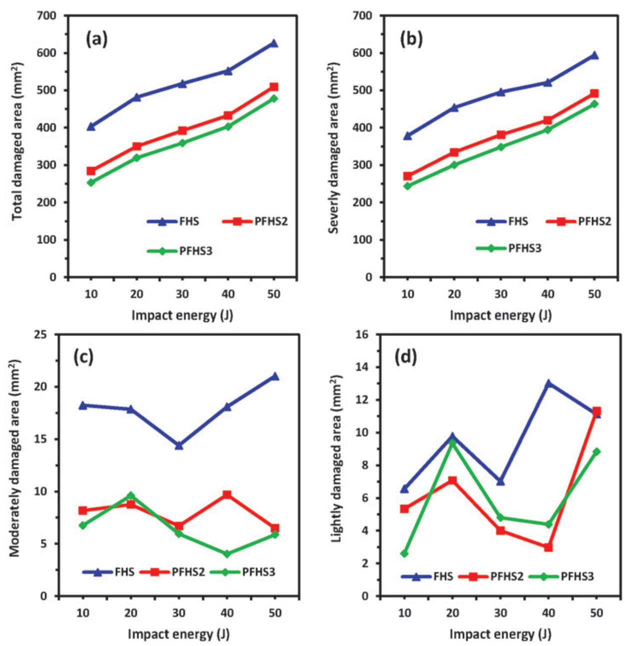


**Figure 5:** Damaged area values classified depending on severity: a) total damaged area, b) severely damaged area, c) moderately damaged area, d) lightly damaged area

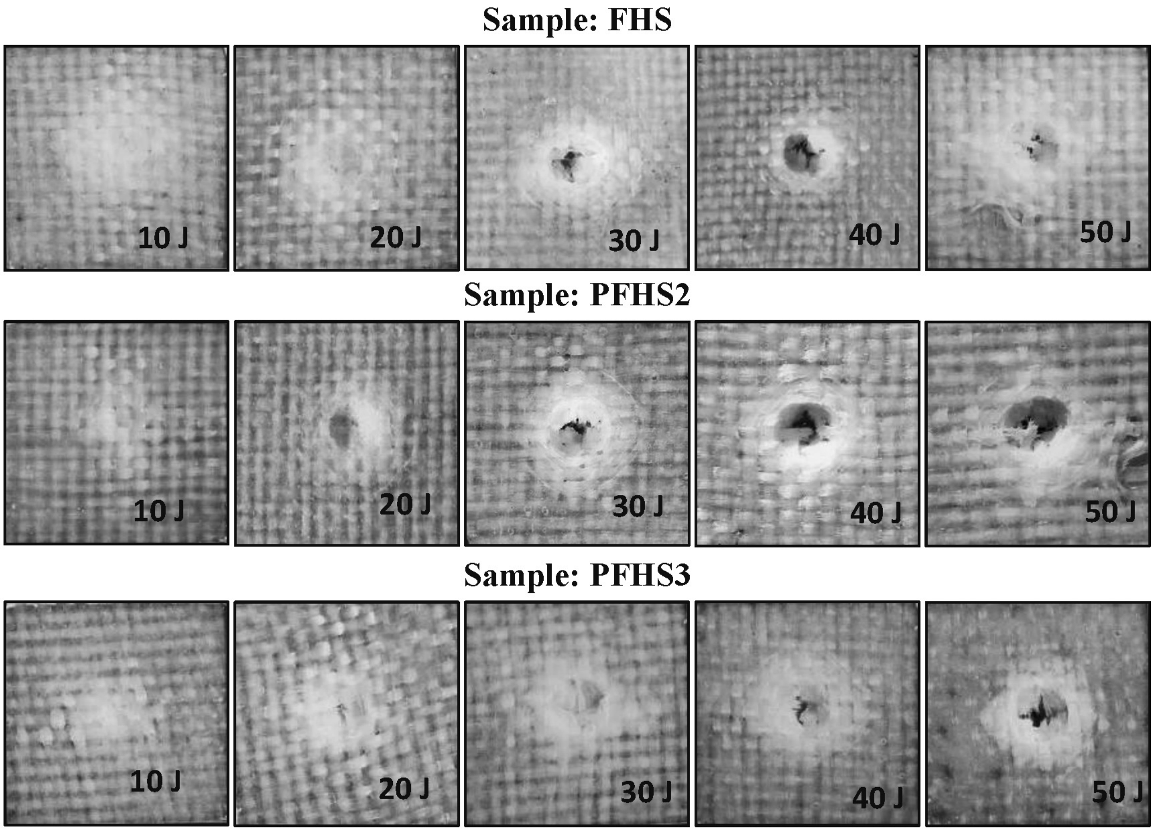


**Figure 6:** Images of polymer sandwich panels (front faces) exhibiting impact damage due to different impact energies of 10–50 J

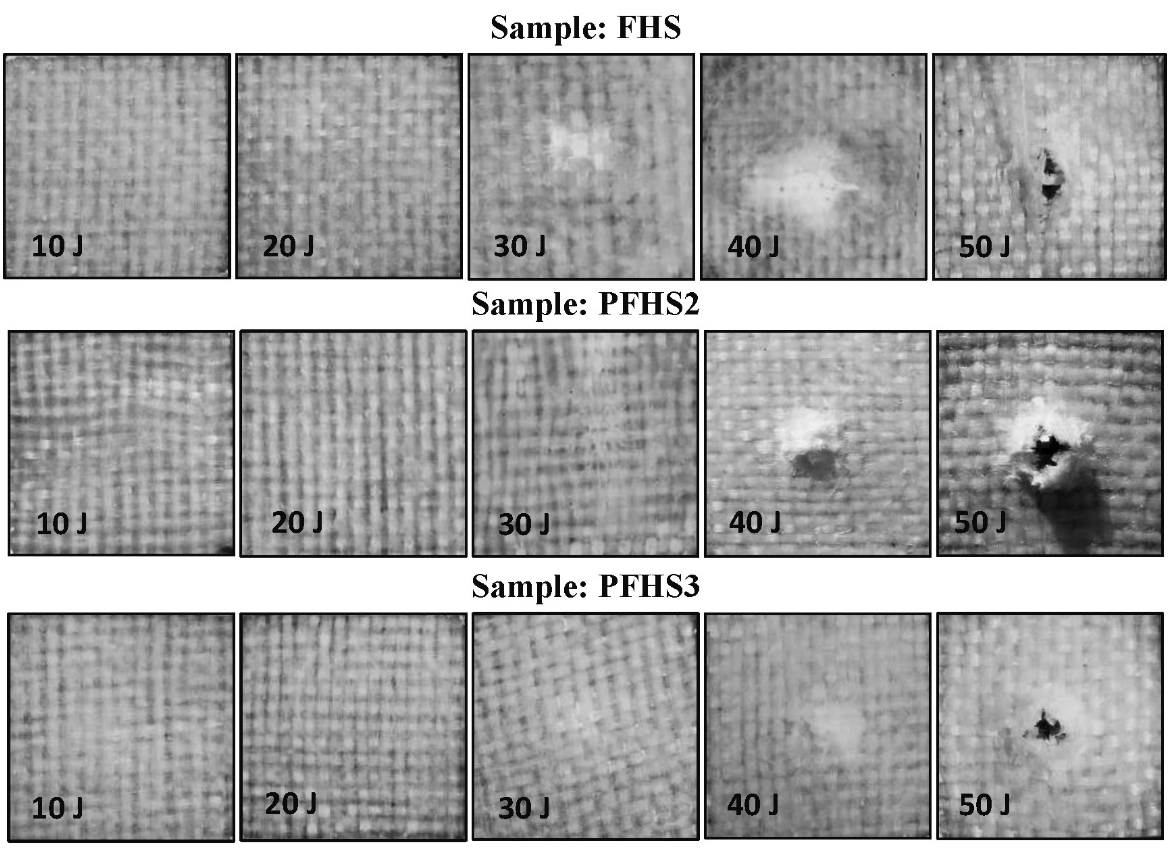


**Figure 7:** Images of polymer sandwich panels (back faces) exhibiting impact damage due to different impact energies of 10–50 J

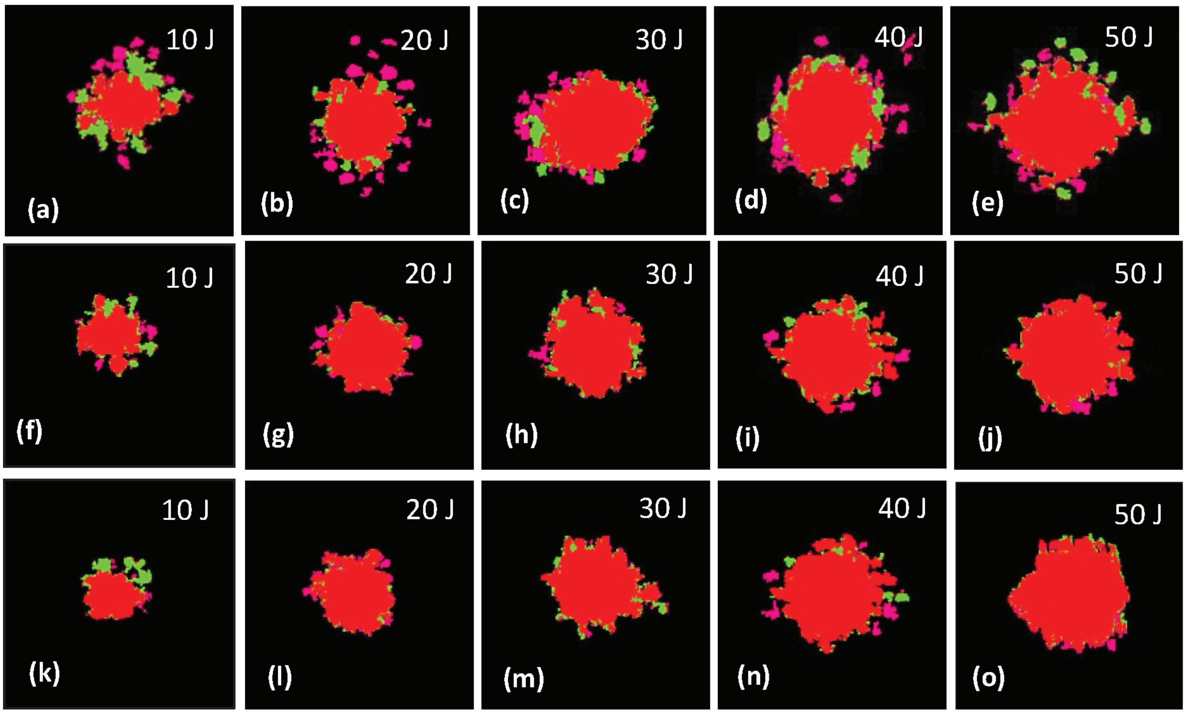


**Figure 8:** Digital images of the damage in different samples: a–e) FHS, f–j) PFHS2, k–o) PFHS3

lightly damaged also increases. Medium and lightly damaged areas are very similar.

### *3.2 Influence of impact energy on different samples*

**Figures 6** and **7** depict typical damage profiles observed on FHS and PFHS specimens' front and back faces subsequent to impact loading. Notably, failure modes observed on PFHS2 and PFHS3 specimens exhibit similarities. Upon visual inspection of the specimens subjected to a 10 J impact, the damage is predominantly confined to localized delamination at the point of impact on the top face sheet for both FHS and PFHS panels. Elevating the impact energy to 20 J introduces a minor dent at the impact site on both FHS and PFHS panels. At 30 J, significant damage is evident, with both face sheet damage and foam core crushing observed in both FHS and PFHS panels. At this energy level, the impact-induced damage extends beyond mere delamination, including core rupturing. Intriguingly, while no visible damage is observed on the back face of PFHS panels, delamination from the core is noticeable in FHS panels.

Increasing the impact energy to 40 J exacerbates the damage, with both face sheets experiencing damage and the core undergoing crushing. Notably, the front face sheet is perforated, while the back face sheet delaminates outward. The increase in delamination, typically an internal damage indicator, suggests significant internal damage. Comparatively, the damage incurred under a 50 J impact load surpasses that under a 40 J load, with both FHS and PFHS specimens exhibiting through-thickness perforation. An analysis of the sandwich panel's front face reveals that voids in the top face sheet indicate penetration points, accompanied by circumferential fractures around the impact site in both FHS and PFHS panels. Additionally, radial perforation is observed on the rear face sheet, with extensive delamination noted across all panels, particularly on the back face sheet.

### *3.3 Digital image processing of damage using MATLAB*

**Figure 8** shows that at impact energies of 10–50 J, the severity of damage to the PFHS panel is consistently lower compared to the FHS panel. On the FHS panel, the outward spread of rose and green colours, representing moderate and light damage, indicates delamination growth, a phenomenon absent in the PFHS panel. This reduction in delamination is attributed to the robust interface bonding between the faces and core, augmented by pins.[31] Contrary to the FHS panel, the damage of the PFHS panel is primarily localized to the impact zone, with delamination growth curtailed by the strengthened interface bonding facilitated by the incorporated pins.[32]

### *3.4 Microscopic investigation*

**Figures 9** and **10**, presenting a microscopic analysis (optical) of impact-tested specimens, reveal notable findings. At the 10 J energy level, neither FHS nor PFHS panel exhibits evidence of fiber cracking. Upon increasing the impact energy to 20 J, both FHS and PFHS panel exhibit fracture lines, matrix cracks, and fiber cracks surrounding the impact zone on the front face, while no damage is apparent on the back face. Transitioning to the 30 J impact energy, damage becomes evident on both the face sheets and core of both FHS and PFHS panel. The damage on the front face resembles that at 20 J. However, a microscopic view of the back face of the FHS panel reveals delamination and minor cracks, contrasting

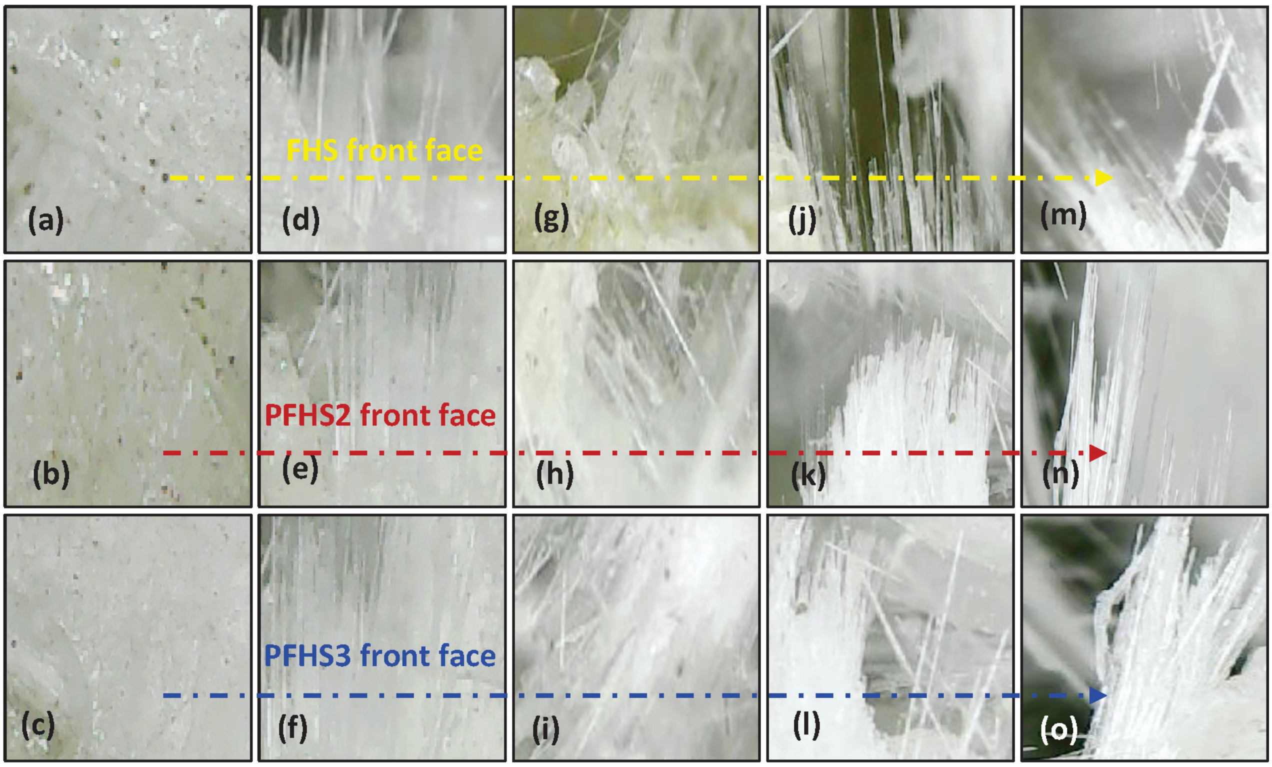


**Figure 9:** Microstructural images of the samples (front faces) at: a–c) 10 J, d–f) 20 J, g–i) 30 J, j–l) 40 J, m–o) 50 J

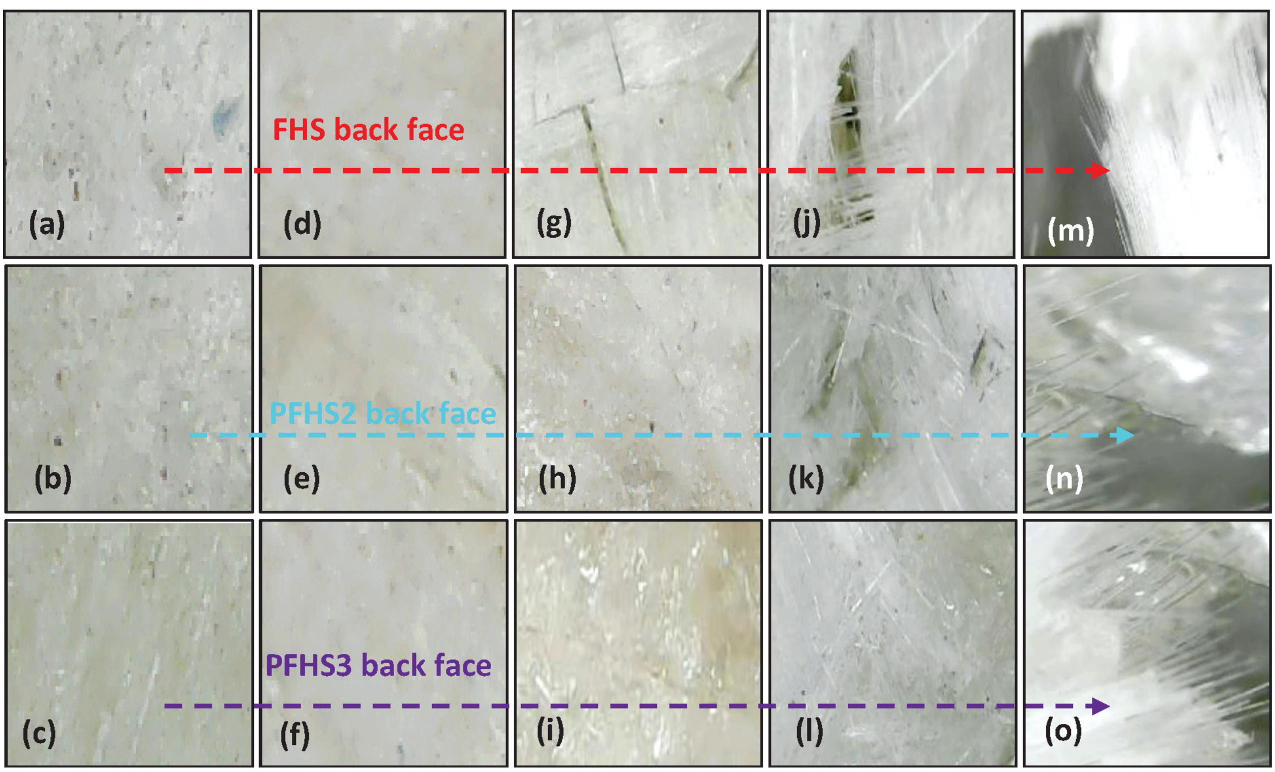


**Figure 10:** Microstructural images of the samples (back faces) at: a–c) 10 J, d–f) 20 J, g–i) 30 J, j–l) 40 J, m–o) 50 J

the PFHS panel, which shows no damage. At the 40 J impact energy level, a microscopic examination of the front face of both FHS and PFHS panel reveals fiber breakage and core rupture. On the back face of the FHS panel, delamination and fiber breakage occur, while only delamination is observed on the PFHS panel. Upon subjecting the specimens to the 50 J impact, both FHS and PFHS specimen sustained more severe damage compared to the damage incurred at the 40 J impact energy level. Microscopic examination confirms fiber fracture and core rupture of both panel types.

## 4 CONCLUSIONS

This study investigated the damage tolerance and failure mechanisms of polyester pin-incorporated PFHS in comparison to FHS under LVI testing. The study confirms the effectiveness of the polyester pin reinforcement in improving the impact resistance of foam-filled honeycomb sandwich panels and validates the use of image processing as a robust tool for precise damage evaluation. The following conclusions were drawn:

The use of MATLAB-based image processing was proved to be a practical, accurate, and cost-effective approach as it enabled precise determination of an impact-damaged area, overcoming the inaccuracies associated with traditional visual inspection methods.

The proposed method demonstrated that the exact damaged area is, on average, 35 % smaller than the maximum damaged area estimated with conventional methods, highlighting the limitations of relying solely on the maximum damage diameter.

The damaged area increased with increasing impact energy for both PFHS and FHS panels. However, PFHS panels exhibited significantly smaller damaged areas at all energy levels, emphasizing their superior damage resistance.

PFHS panels demonstrated significantly improved structural performance and damage tolerance compared to FHS panels. This enhancement was achieved with a minimal weight increase, making them a viable option for applications requiring lightweight yet highly durable sandwich structures.

The polyester pin reinforcement in PFHS panels enhanced interlayer crack resistance by establishing a strong interface between the faces and the core, minimizing the extent of damage even under high-energy impacts.

## Declaration

Conflict of interest: No conflict of interest.
Funding: No funding was received.

## 5 REFERENCES

[1] R. S. Jayaram, V. A. Nagarajan, K. P. V. Kumar, Mechanical performance of polyester pin-reinforced foam-filled honeycomb sandwich panels, Sci Eng Compos Mater, 25 (**2018**) 25, 797–805

[2] R. S. Jayaram, S. S. Murugan, P. V. Prasanth, et al., Evaluation of damage area on low-velocity impact tested AA3003 sandwich panels using digital image analysis: A novel method, J Inst Eng (India) Ser D, (**2022**), doi:10.1007/s40033-022-00382-6

[3] H. Kim, J. C. Halpin, G. K. Defrancisci, Impact damage of composite structures, In: Long-term durability of polymeric matrix composites, Boston, MA: Springer, (**2012**), 143–180

[4] J. Susainathan, F. Eyma, E. De Luycker, et al., Experimental investigation of compression and compression after impact of wood-based sandwich structures, Compos Struct, 220 (**2019**), 236–249

[5] P. Majumdar, D. Srinivasagupta, H. Mahfuz, et al., Effect of processing conditions and material properties on the debond fracture toughness of foam-core sandwich composites: experimental optimization, Compos Part A Appl Sci Manuf, 34 (**2003**), 1097–1104

[6] N. Mitra, B. R. Raja, Improving delamination resistance capacity of sandwich composite columns with initial face/core debond, Compos B Eng, 43 (**2012**), 1604–1612

[7] M. Z. Hassan, S. M. Sapuan, Z. A. Rasid, et al., Impact damage resistance and post-impact tolerance of optimum banana-pseudo-stem-fiber-reinforced epoxy sandwich structures, Appl Sci (Basel), 10 (**2020**), 684

[8] M. H. Khan, M. Elamin, B. Li, et al., X-ray micro-computed tomography analysis of impact damage morphology in composite sandwich structures due to cold temperature arctic condition, J Compos Mater, 52 (**2018**), 3509–3522

[9] C. Sergi, F. Sarasini, P. Russo, et al., Effect of temperature on the low-velocity impact response of environmentally friendly cork sandwich structures, J Sandw Struct Mater, 24 (**2022**), 1099–1121

[10] A. Saifullah, L. Wang, A. Barouni, et al., Low velocity impact (LVI) and flexure-after-impact (FAI) behaviours of rotationally moulded sandwich structures, J Mater Res Technol, 15 (**2021**), 3915–3927

[11] N. Geren, D. C. Acer, C. Uzay, et al., The effect of boron carbide additive on the low-velocity impact properties of low-density foam core composite sandwich structures, Polym Compos, 42 (**2021**), 2037–2049

[12] C. Zhang, Y. Rao, Z. Li, et al., Low-velocity impact behavior of interlayer/intralayer hybrid composites based on carbon and glass non-crimp fabric, Materials (Basel), 11 (**2018**), 2472

[13] S. Alsubari, M. Y. M. Zuhri, S. M. Sapuan, et al., Potential of natural fiber reinforced polymer composites in sandwich structures: A review on its mechanical properties, Polymers (Basel), 13 (**2021**), 423

[14] R. Studziński, Z. Pozorski, Experimental and numerical analysis of sandwich panels with hybrid core, J Sandw Struct Mater, 20 (**2018**), 271–286

[15] I. E. Tabrizi, A. Kefal, J. S. M. Zanjani, et al., Experimental and numerical investigation on fracture behavior of glass/carbon fiber hybrid composites using acoustic emission method and refined zigzag theory, Compos Struct, 223 (**2019**), 110971

[16] C. Berggreen, B. C. Simonsen, K. K. Borum, Experimental and numerical study of interface crack propagation in foam-cored sandwich beams, J Compos Mater, 41 (**2007**), 493–520

[17] H. Ahmadi, M. Ekrami, H. Sabouri, et al., Experimental and numerical investigation on the effect of projectile nose shape in low-velocity impact loading on fiber metal laminate panels, Proc Inst Mech Eng G J Aerosp Eng, 233 (**2019**), 3665–3679

[18] Z. Qin, L. Wei, M. Zhang, et al., The effects of core machining configurations on the mechanical properties of cores and sandwich structures, Materials (Basel), 15 (2**0**22), 521

[19] P. V. Prasanth, M. E. Sahaya Raj, J. T. W. Jappes, et al., Study of matrix modifications by nano-clay on the mechanical properties of AA3003 honeycomb sandwich panels, Proc Inst Mech Eng Part C, 236 (**2022**), 7974–7983

[20] A. Eyvazian, M. Moeinifard, F. Musharavati, et al., Mechanical behavior of resin pin-reinforced composite sandwich panels under quasi-static indentation and three-point bending loading conditions, J Sandw Struct Mater, 23 (**2021**), 2127–2145

[21] B. Abdi, S. Azwan, M. R. Abdullah, et al., Flatwise compression and flexural behavior of foam core and polymer pin-reinforced foam core composite sandwich panels, Int J Mech Sci 88, (**2014**), 138–144

[22] H. B. Kaybal, H. Ulus, V. Eskizeybek, et al., An experimental study on low velocity impact performance of bolted composite joints part 1: Influence of halloysite nanotubes on dynamic loading response, Compos Struct, 258 (**2021**), 113415

[23] D. A. Drake, R. W. Sullivan, S. B. Clay, et al., Influence of stitching on the fracture of stitched sandwich composites, Compos Part A Appl Sci Manuf, 145 (**2021**), 106383

[24] M. Safarabadi, M. Haghighi-Yazdi, M. A. Sorkhi, et al., Experimental and numerical study of buckling behavior of foam-filled honeycomb core sandwich panels considering viscoelastic effects, J Sandw Struct Mater, 23 (**2021**), 3985–4015

[25] M. V. Hosur, M. Abdullah, S. Jeelani, Manufacturing and low-velocity impact characterization of foam filled 3-D integrated core sandwich composites with hybrid face sheets, Compos Struct, 69 (**2005**), 167–181

[26] C. C. Tsao, H. Hocheng, Computerized tomography and C-Scan for measuring delamination in the drilling of composite materials using various drills, Int J Mach Tools Manuf, 45 (**2005**), 1282–1287

[27] R. Kumpati, W. Skarka, S. K. Ontipuli, Current trends in integration of nondestructive testing methods for engineered materials testing, Sensors (Basel), 21 (**2021**), 6175

[28] R. S. Jayaram, V. A. Nagarajan, K. P. V. Kumar, Polyester pinning effect on flexural and vibrational characteristics of foam filled honeycomb sandwich panels, Lat Am J Solids Struct, 14 (**2017**), 1314–1326

[29] R. S. Jayaram, V. A. Nagarajan, K. P. Vinod Kumar, Compression and low velocity impact response of sandwich panels with polyester pin-reinforced foam filled honeycomb core, J Sandw Struct Mater, 21 (**2019**), 2014–2030

[30] R. S. Jayaram, V. A. Nagarajan, K. P. V. Kumar, Low velocity impact and compression after impact behaviour of polyester pin-reinforced foam filled honeycomb sandwich panels, J Sandw Struct Mater, 24 (**2022**), 157–173

[31] A. Nanayakkara, S. Feih, A. P. Mouritz, Experimental impact damage study of a z-pinned foam core sandwich composite, J Sandw Struct Mater, 14 (**2012**), 469–486

[32] A. K. J. Al-Shamary, R. Karakuzu, O. Özdemir, Low-velocity impact response of sandwich composites with different foam core configurations, J Sandw Struct Mater, 18 (**2016**), 754–768